Synthesis and characterization of europium activated lanthanum oxysulphide by sol- combustion method.

Ali AG, Dejene BF[a*] and Swart[b] HC.
[a]Department of Physics, University of the Free State (Qwaqwa Campus), Private Bag X13, Phuthaditjhaba, 9866, South Africa.
[b]Department of Physics, University of the Free State, P.O. Box 339, Bloemfontein, 9300, South Africa.
* Corresponding author: Tel: +27 58 718 6259; Fax: +27 58 718 5444; E-mail: aliag@qwa.ufs.ac.za

Abstract
Sol-combustion synthesis was used to obtain nanocrystalline La_2O_2S red-emitting phosphors. X-ray diffraction (XRD) was employed to determine that the powders in the as-synthesized samples were crystalline. Upon increasing La/S molar ratios, the crystallinity in the nanosized particles increased, which resulted in a higher photoluminescence emission intensity of these phosphors. Fourier-transform infrared spectrometry analysis showed that there is a negligible difference in the absorbed impurities with various molar ratios. Hence, it was concluded that the La/S molr ratio plays an important role in the luminescence intensity of these phosphors.

I. Introduction

Lanthanide (La) oxysulfides with high thermal and chemical stability are known as wide-bang gap (4.6-4.8 eV) materials suitable for doping ion activation [1]. Compared with the lanthanide oxides, oxysulfide is a more efficient phosphor with a broader excitation band. Therefore, the lanthanide oxysulfides become a very important family of inorganic materials that have high potential for applications in various fields, such as color television picture tubes [2], radiographic imaging [3], field emission displays [4, 5] and long-lasting phosphorescence [6-8]. Among them, Eu^{3+} activated lanthanide oxysulfide has been extensively investigated due to its very efficiency to be used as a red phosphor applied in television picture tubes.

In this paper we investigate the effect of varying fuel to host ratio in the luminescence intensity of europium activated lanthanum oxysulphide.

2. Experimental.

La $(NO_3)_3.6H_2O$, NH_2CSNH_2, $Eu(NO_3)_3.6H_2O$, ethanol, distilled water were mixed in required stoichiometric ratios and dissolved by stirring using magnetic stirrer for 5 -10 minutes. Mixture heated in an air tube furnace to ignition temperature of 400^0c. White foamy product obtained after combustion reaction. Several samples with different La/S molar ratios were then prepared via similar route. The formation mechanism for La_2O_2S and La (OH)- CO_3 was proposed.

The Photoluminescence spectrum was investigated by Cary Eclipse fluorescent spectrophotometer equipped with a 150 W xenon lamp as an excitation source with the slit of

1. 0 nm and scan speed of 240 nm min. To determine the average particle diameter and the phase of the samples, X-ray powder diffraction spectra were measured with a D8 Bruker Advanced AXS GmbH X-ray diffractometer using Cu *Ka* radiation at a wavelength of 0.154056 nm, the size and morphology of the as-prepared particles were carried out by using Scanning electron microscope, SHIMADZU SSX-550 SPERSCAN.

3. Results and Discussion.

3.1. Crystal structure.

Figure 1 shows that the XRD pattern of the La_2O_2S powders synthesized by the Sol-Combustion process at 400 °C. Majority of the peaks can be indexed as the pure hexagonal La_2O_2S phase

with cell constants *a*) 0.4047 nm, *c*) 0.6944 nm, which are close to the reported data (JCPDS Cards File: 27-0263)

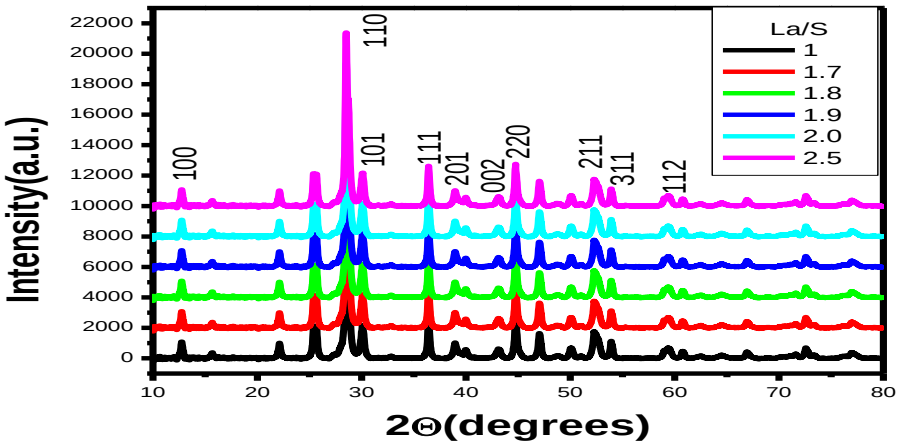

Figure1. X- ray diffraction of La_2O_2S with different La/S ratio

The average crystalline size of the La_2O_2S particles calculated using most intense reflection at 2θ= 28.596° are tabulated in table 1. Estimated according to the Scherrer's equation, the average crystalline size of the powders is determined to be 180 nm, which is basically in consistent with the crystalline size estimated by SEM images.

La/S	2θ°	$\beta 1/_2$	Grain size(nm)
1.0	28.586	0.37861	178
1.7	28.627	0.42738	175
1.8	28.608	0.4519	189
1.9	29.988	2.4113	175
2.0	3.0272	2.2562	182
2.5	33.657	2.0459	184

Table 1

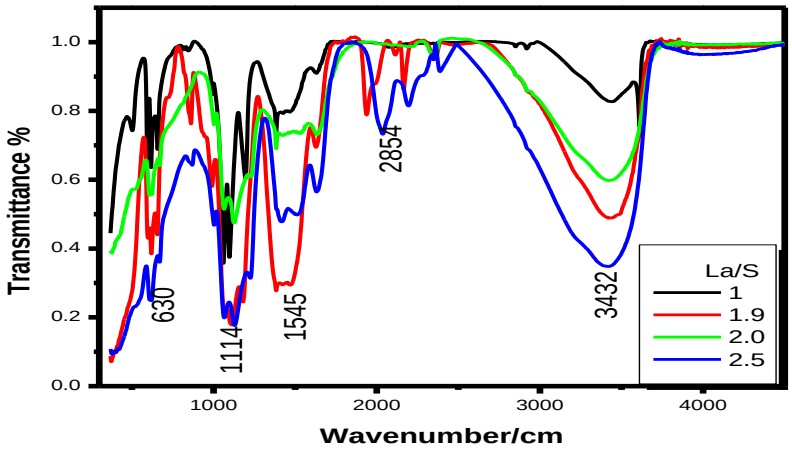

Figure 2 Fourier-transform infrared of the as-prepared La_2O_2S: Eu^{3+} powders.

To identify the presence of La_2O_2S, we employed FTIR studies in the wave number range 400 cm^{-1} to 4500 cm-1. From fig. 2 above its revealed that the strong broad absorption band at 3500 cm-1 is due to water [12]. The weaker absorption bands at 1114, 1545 and 2854 cm-1 are due to host La_2O_2S, since the dopant have no effect. The presence of the vibrational peaks at around 630 cm-1 corresponds to La-O stretching modes [13], because by increasing La/S molar ratios the bonds also increase.

3.2 Morphology

Figure 3 shows SEM images of La_2O_2S: Eu^{3+} nanocrystalline powders. It is obvious that all the powders yield nanoparticles and they tend to aggregate together. The images showed that the morphology consisted of a foamy, porous agglomeration and a continuous three-dimensional network. The agglomerates ranged in size between 5 and 20 mm, while the primary particles ranged in size between 175 to 184 nm. The average sizes of the nanoparticles are about 180 nm.

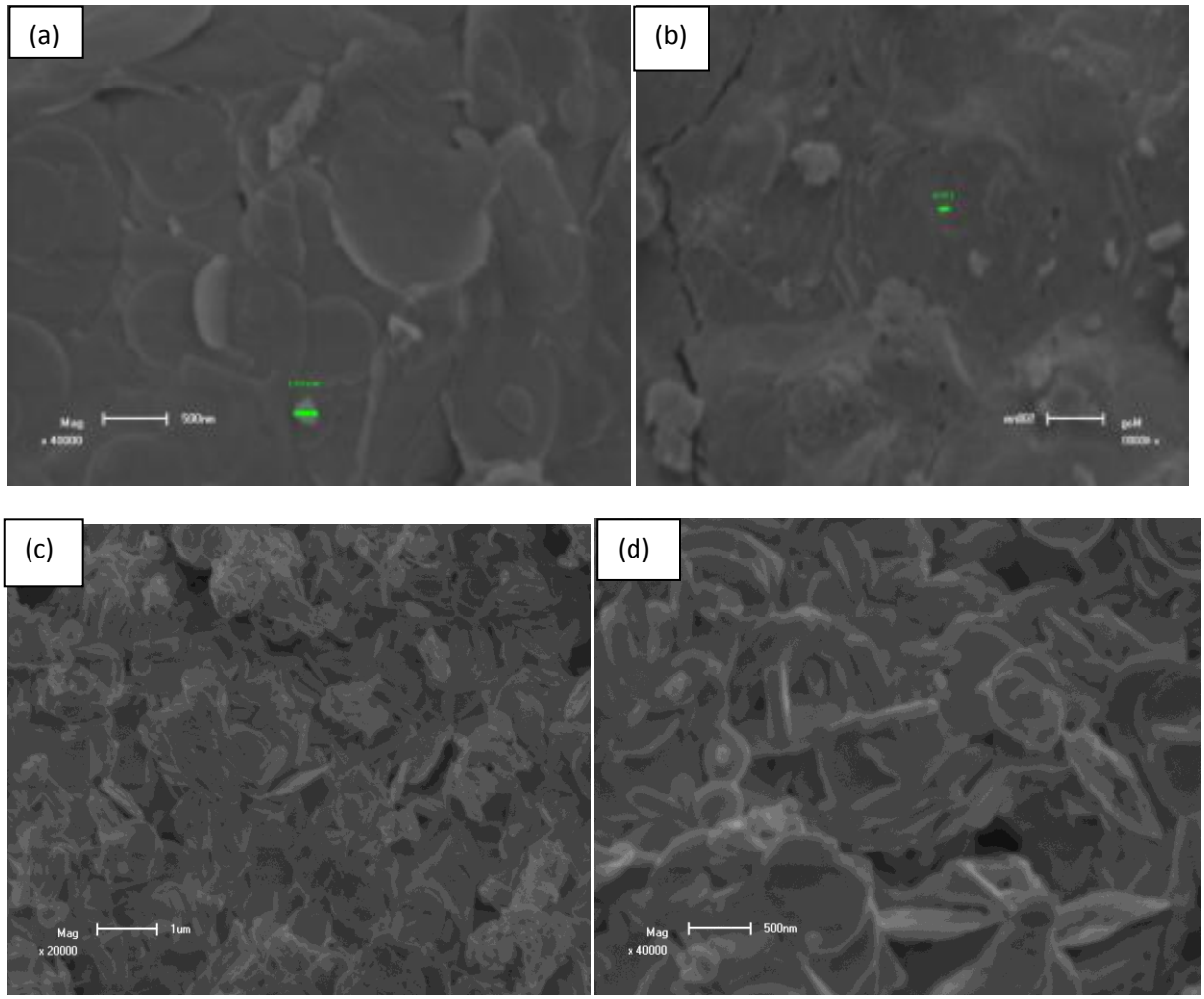

Fig.3(a)-----(b)----(c)-----(d)----(e)----- SEM micrographs of the as-prepared La_2O_2S: Eu^{3+} powders at 40000 field of view.

3.3 Photoluminescence

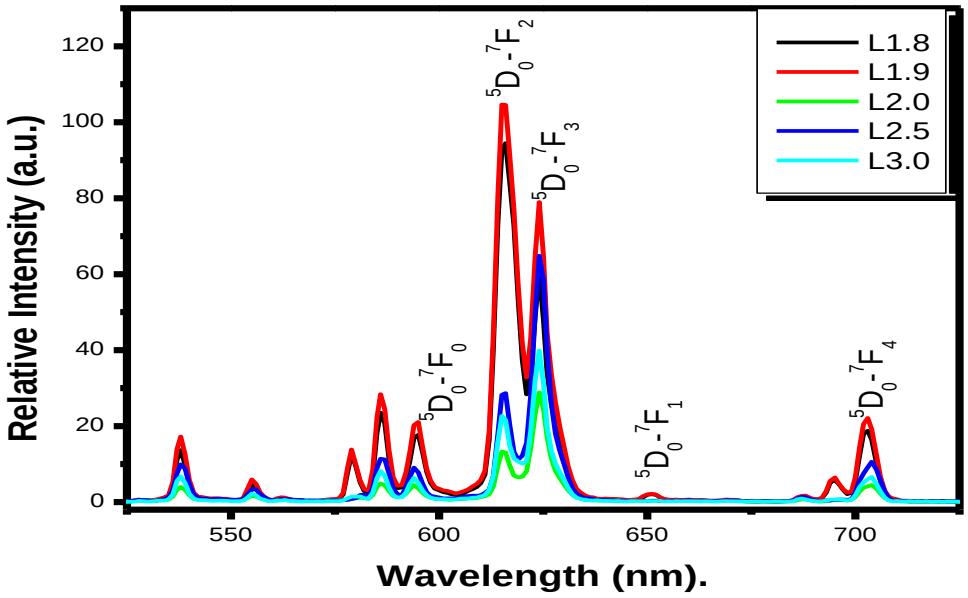

Fig.4 PL emission spectra of La_2O_2S with different La/S molar ratios.

Fig.4. shows the emission spectra of Eu^{3+} which are assigned to $^5D_0 \rightarrow {}^7F_{0,\,1,2,3,4}$ transitions of Eu^{3+}. There is no obvious difference in all the emissions of samples doped with Eu^{3+} except the peak position shifted at La/S molar ratios of 2.5 at 615nm wavelength. The peak intensity quenches at a wavelength of 624nm.

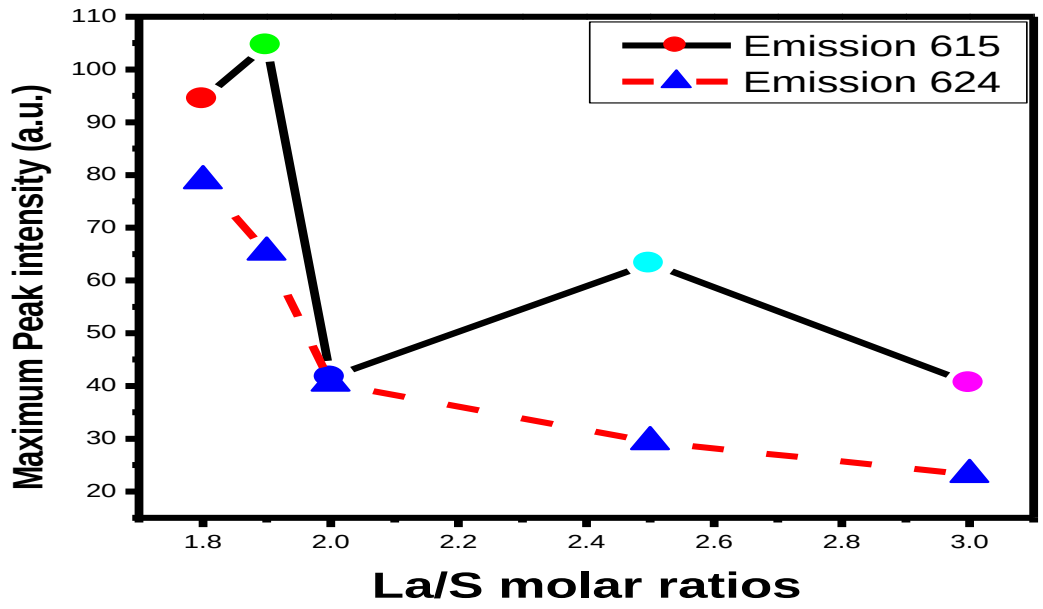

Fig.5 Graph of La/S molar ratio versus maximum peak intensity.

The graph of maximum PL intensity of the as-prepared powders as a function of La/S molar ratios is shown in Fig.5. The emission peak intensity decreased when the La/S molar ratio increased, and a maximum value was found when La/S= 1.9, thereafter the emission intensity quenches gradually. Persistent luminescence curves of the phosphor powders were shown in the fig. 6. It can be seen from the curve that the powders showed differences in initial intensity and medium persistence when the powders were efficiently activated by UV lamp. The results indicate that the initial luminescence intensity and the decay time of phosphors are enhanced with a decrease in the La/S molar ratios..

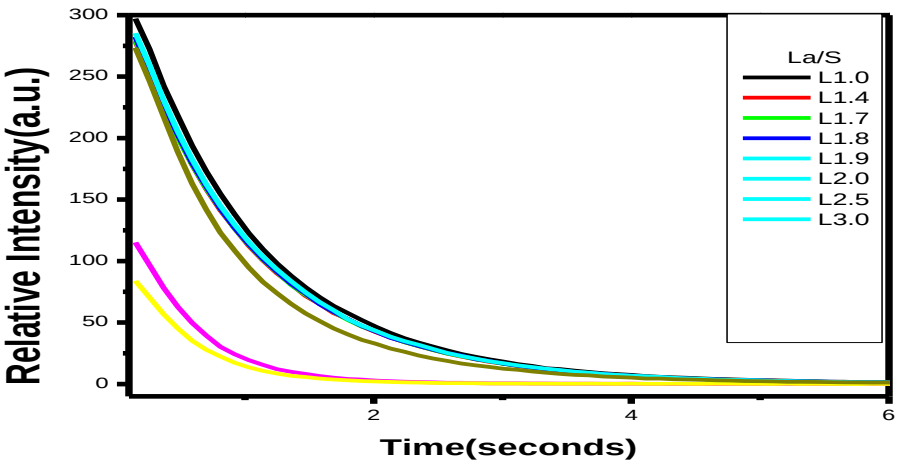

Fig.6 Afterglow characteristics of La_2O_2S with different La/S molar ratios.

The decay behavior can be analyzed by curve fitting, relying on the following triple exponential equation:
$I= A_1 \exp(-t/\tau_1) + A_2 \exp(-t/\tau_2) + A_3 \exp(-t/\tau_3)$. ---------- (1)
Where I is phosphorescence intensity, A_1, A_2, and A_3 are constants, t is time, τ_1, τ_2, and τ_3 are decay constants, deciding the decay rate for rapid, medium and slow exponentially decay components, respectively. The fitting results of parameters t_1, t_2 and t_3 are listed in Table 2 below.

La/S	1.0	1.4	1.7	1.8	1.9	2.0	2.5	3.0
Components				Decay	Const.(s)			
Fast(τ_1)	0.97	0.95	0.91	0.88	0.82	0.76	0.68	0.54
Medium(τ_2)	1.08	0.99	0.97	0.87	0.75	0.63	0.58	0.46
Slow(τ_3)	3.43	3.23	3.17	3.06	2.96	2.75	2.14	1.98

Table 2 Results for the fitted decay curves of the phosphor powders with different La/S molar ratios.

Three components namely slow, medium and fast are responsible for the persistent luminescence from the synthesized phosphor. A trend can be observed (fig.7) that the decay constants of the phosphors decrease gradually with the increasing La/S molar ratios.

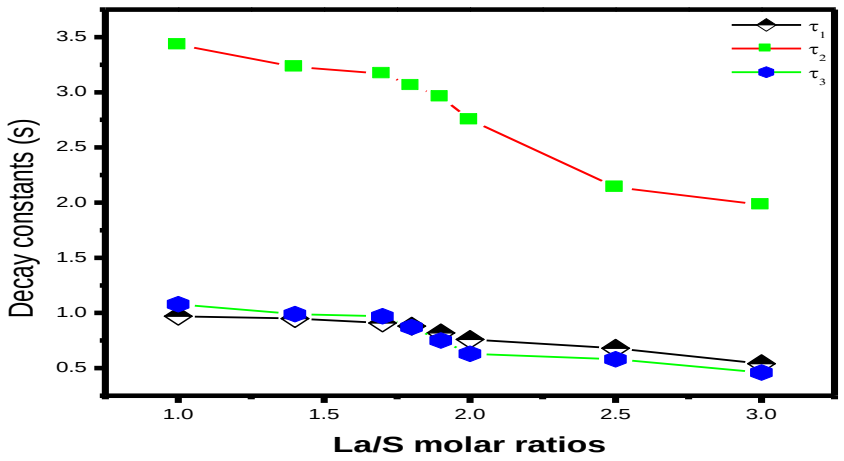

Fig.7 Graph of decay constants verse La/S molar ratios.

4. Conclusions

The XRD pattern of as-synthesized powder revealed that the La_2O_2S phase crystallized directly from the combustion reaction with fuel to oxidizer ratios at ignition temperatures of 400^0C. Powders synthesized with a lower La/S ratio, were contaminated by residual carbonaceous material. De-hydration of the reactants was crucial for the successful synthesis of the oxysulfide phase. SEM images of as-synthesized powders showed that the morphology consisted of a foamy, porous agglomeration and a continuous three-dimensional network.

Acknowledgement

The authors would like to acknowledge National Research Foundation (NRF) of South Africa and University of the Free State (UFS) for financial support.

References

[1] P.Majewski , M.Rozumek, H.Schluckwerder, F. Aldinger, Int. J. Inorganic Mater. 3 (2001) 1343.
[2] Garcia-Murillo, C. Luyer, C. Garapon, C. Dujardin, E. Bernstein, C. Pedrini, J. Mugnier, Opt. Mater. 19 (2002) 161.
[3] W. Jungowska, J. Thermal Anal. Calorimetry 60 (2000) 193.
[4] T, Feldmann, Justel, C. Ronda, P. Schmidt, Adv. Funct. Mater. 13 (7) (2003) 511.
[5] Y. Nakanishi, in: Proc. of the III Int. meeting on Information Display, IMID, Daegu, Korea, 2003, p. 203.
[6] V.L. Levshin, M.A. Konstantinova, E.A. Trapeznikova, On the application of rare-earth elements in the chemistry of phosphors, in: Rare-earth Elements, USSR AN Publishing, Moscow, 1959, p. 314.
[7] T. Hisamune, Technical trend of phosphors for plasma display panels, in: Proceedings of the 9th International Display Workshops, 2002, p. 685.
[8]. T. Justel, H. Nikol and C. Ronda. Angew. Chem. Int. 37 (1998), 3085.
[9]. S. Shionoya and W.M. Yen, Editors, Phosphor Handbook, CRC Press, Boca Raton, FL (1998).
[10]. C.F. Bacalski, M.A. Cherry, G.A. Hirata, J. Mckittrick, J. Mourant, J. Soc. Inf. Display (Suppl-1) (2000) 93.
[11]. G.C. Kim, H.L. Park and T.W. Kim. Mater. Res. Bull. 36 (2001), p.1603.
[12]. M. Kottaisamy, D. Jeyakumar, R. Jagannathan and M.M. Rao. *Mater. Res. Bull.* **31** (1996), p. 1013.
[13]. L.E. Shea, J. Mckittrick, O.A. Lopez, E. Sluzky and M.L. Phillips. *J. Soc. Inf. Display* **5** (1997), p. 117.
[14]. J. McKittrick, L.E. Shea, C.F. Bacalski and E.J. Bosze. *Displays* **19** (1999), p. 169.
[15]. K.C. Patil and S. Ekambaram. *J. Alloys Compounds* **248** (1997), p. 7.